IEEE Access
Multidisciplinary ⋮ Rapid Review ⋮ Open Access Journal

Received September 5, 2019, accepted October 14, 2019, date of publication October 22, 2019, date of current version November 4, 2019.

*Digital Object Identifier 10.1109/ACCESS.2019.2948963*

# Adaptive Terminal Sliding Mode Control for Reentry Vehicle Based on Nonlinear Disturbance Observer

**BINGHE AN, BO WANG, YONGJI WANG, (Member, IEEE), AND LEI LIU**
School of Artificial Intelligence and Automation, Huazhong University of Science and Technology, Wuhan 430074, China
National Key Laboratory of Science and Technology on Multispectral Information Processing, Huazhong University of Science and Technology, Wuhan 430074, China

Corresponding author: Bo Wang (wb8517@hust.edu.cn)

This work was supported in part by the National Natural Foundation of China under Grant 6187319 and Grant 61803162.

**ABSTRACT** The movement of reentry vehicle is disturbed by the atmospheric environment and changes of aerodynamic parameters. In this paper, an adaptive terminal sliding mode control method based on nonlinear disturbance observers is proposed, which is used to control the attitude of the reentry vehicle. Firstly, the attitude control system is divided into an attitude angular control loop and an angular velocity control loop. Then, novel finite time convergence nonlinear disturbance observers are designed to estimate lumped disturbances. In the design of control law, the super-twist algorithm is used to make the proposed terminal sliding mode variables converge to the origin within a finite time and reduce the chattering of the controller. The estimated value of disturbance is considered in the controller to attenuate the effect of disturbances on the vehicle. Last, the algorithm proposed is applied to reentry vehicle and a good performance can be obtained. The effectiveness and superiority of the proposed algorithm is demonstrated by numerical simulations.

**INDEX TERMS** Reentry vehicle, attitude control, nonlinear disturbance observer, terminal sliding mode, super twist algorithm.

## I. INTRODUCTION

The velocity of the reentry vehicle is fast, and the flight is affected by wind disturbance, atmospheric density and change in the Earth's gravitational force [1]. The aerodynamic parameters of vehicles are time-varying because aerodynamic parameters are affected by altitude and velocity changes. As a result, the movement of the reentry vehicle has obvious nonlinearity, coupling, and uncertainty characteristics [2]. Attitude control plays an important part in the reentry vehicle control system. Achieving a precise attitude control can provide enough aerodynamic force to ensure that the vehicle can stably track guidance instructions.

The vehicle attitude control methods commonly used include auto disturbance rejection control [3], back-stepping control [4], and sliding mode control(SMC). SMC is a nonlinear control method proposed by former Soviet scholar Emelyanov. The main advantage of the sliding mode control method is that it is not sensitive to external disturbances and uncertainties [5]. With the concept of reaching law, dynamic sliding mode, and high-order sliding mode [6] being proposed, the sliding mode control theory has been further developed. Many scholars have applied the sliding mode control method in the vehicles field. Munoz *et al.* [7] used the improved second-order sliding mode method in the attitude control problem of the quadrotors. The experiments were conducted outdoors, and noise was added during the flight of the quadrotors. Using the control law proposed, the attitude angles of the vehicle can effectively track the desired signals, although with disturbances, which proves the feasibility of the sliding mode control method in practical applications. Tian *et al.* [8] proposed a dynamic sliding variable method for the attitude tracking problem of the reusable launch vehicle. The initial sliding variable was designed which was set at the origin from the initial time, so that the arrival phase of the sliding mode control is eliminated, and the global robustness of the system is improved. By adding the relative degrees of the system, the quasi-continue high order sliding mode control laws were used for attitude control of reusable launch vehicles in [9]. However, the higher derivative of system

The associate editor coordinating the review of this manuscript and approving it for publication was Zhiguang Feng.

states and the sliding mode variable need to be obtained for completing the control law. The terminal sliding mode controller(TSMC), which was proposed in [10], is a finite time control method. Due to the good dynamic characteristics of the terminal sliding mode, TSMC was widely used in the robot control problem [11]. Additionally, in [12], the terminal sliding mode controllers were designed for hypersonic flight vehicle in the vertical plane. In the actual flight process, a faster response to attitude angle commands is required. Thus, the terminal sliding mode method has certain advantages. The major factor that discourages sliding mode control applied in actual engineering is that the controller output has severe high-frequency chattering [13], which increased the energy requirements for actuators and may lead to system instability. The commonly used methods to reduce chattering include designing a high-order sliding mode controller, using sigmoid function to replace the sign function [14], and combining fuzzy logic and the sliding mode control [15]. However, when the sign function is replaced by sigmoid function, the control accuracy is reduced in the presence of disturbances. In addition, using fuzzy logic methods requires great control experience in advance [16]. The super-twist algorithm is a kind of sliding mode method, which can weaken the chattering of the controller while ensuring the stability of the system [17]. In [18], the adaptive super-twist control algorithm is proposed for reusable launch vehicles.

The disturbance observer can estimate the disturbance in the system in real time, and the estimated value can be used to compensate for the disturbance. Thus, the robustness of the system can be effectively improved through disturbance observer. In [19], the maneuver of the target is treated as the interference of the system and an extended state observer is designed to estimate the maneuver of the target. In [20], the fault information and disturbances in the manipulator system can be obtained by an composite observer. The finite time convergence disturbance observer and the controller were proposed for vehicle active suspension systems in [21]. The disturbance observer based on the terminal sliding mode was proposed in [22], which can ensure that the estimation error converges in finite time. Another kind of sliding mode disturbance observer was used in the control problem of the reusable vehicle under uncertainties in [23]. Since the reentry flight process is interfered by changes of external environment, it is necessary to design a disturbance observer to improve the robustness of vehicle control system.

On the basis of previous studies, to control the attitude of the reentry vehicle effectively in the presence of disturbances, the adaptive terminal sliding mode control(ATSMC) are proposed in this paper. Firstly, the attitude control system is divided into two loops. The outer loop is the attitude angular tracking loop, and the inner loop is the angular velocity tracking loop. Nonlinear disturbance observers are proposed to estimate the disturbances in each loop. Terminal sliding mode control laws with disturbance compensation are proposed for two loops to ensure the stability of the attitude control system.

The main contributions of this paper are:

1. Nonlinear disturbance observers using new estimation laws are proposed to estimate disturbances during the reentry flight. Using the proposed disturbance observers can ensure that the estimation errors converge in a finite time. The stability of the disturbance observers is proved by the Lyapunov theory.
2. Terminal sliding mode variables are designed to ensure that state errors converge within a finite time. New adaptive control laws based on the super-twist algorithm and the terminal sliding mode variables designed are proposed to control the attitude angles of the reentry vehicle. The estimated values of the disturbances are considered in the control laws to compensate for disturbances adaptively and attenuate the effect of disturbances on the vehicle. The simulation results show that attitude angles can track the command signals stably with better dynamic performance by using the control laws proposed.

The content of the paper is organized as follows: The attitude control model of reentry vehicles and task analysis are given in section II. The nonlinear disturbance observers are proposed in Section III. After that, the adaptive terminal sliding mode control methods are designed for the reentry vehicle, which are presented in section IV. Numerical simulations that prove the performance of the proposed control laws are performed in section V. Section VI is reserved for conclusions.

## II. THE ATTITUDE MOVEMENT MODEL FOR REENTRY VEHICLES AND TASK ANALYSIS

### A. THE ATTITUDE MOVEMENT MODEL FOR REENTRY VEHICLES

The movement characteristics of the reentry vehicle can be described by three kinematic equations and three dynamics equations. According to the movement model established in papers [24], [25], the rotation dynamics equations are described as follows:

$$\begin{aligned} \boldsymbol{I}_0 \begin{bmatrix} \dot{p} \\ \dot{q} \\ \dot{r} \end{bmatrix} &= -\boldsymbol{\Omega} \boldsymbol{I}_0 \begin{bmatrix} p \\ q \\ r \end{bmatrix} + \boldsymbol{M} \\ \boldsymbol{I}_0 &= \begin{bmatrix} I_{xx} & 0 & -I_{xz} \\ 0 & I_{yy} & 0 \\ I_{xz} & 0 & I_{zz} \end{bmatrix}, \\ \boldsymbol{\Omega} &= \begin{bmatrix} 0 & -r & q \\ r & 0 & -p \\ -q & p & 0 \end{bmatrix} \end{aligned} \tag{1}$$

where $\boldsymbol{I}_0$ is the nominal moment of inertia matrix. $p, q$ and $r$ represent roll, pitch, and yaw rate, respectively. $\boldsymbol{M} = [M_x, M_y, M_z]^{\mathrm{T}}$ is the control torque vector. $M_x, M_y$ and $M_z$ are roll torque, yaw torque and pitch torque, respectively.

The flight of the reentry vehicle is affected by atmospheric conditions and the change of the gravitational force, thus, it is necessary to consider external disturbances and uncertainties in the motion equation. The dynamics equation is

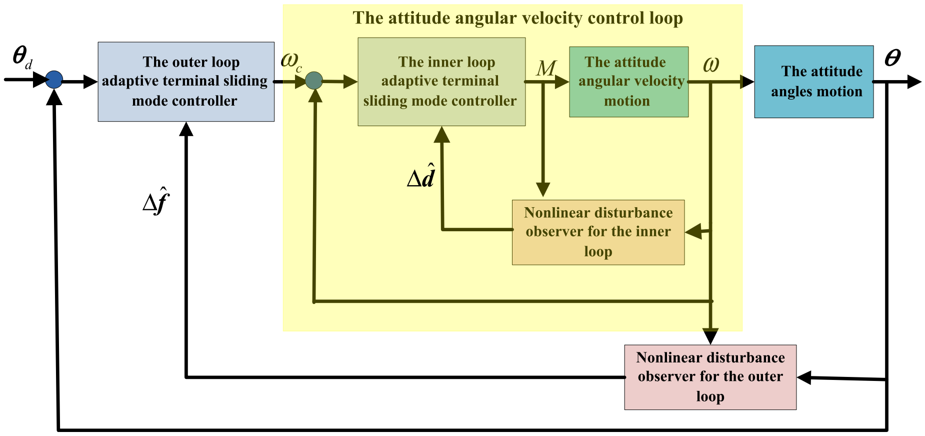


**FIGURE 1.** Attitude control system structure.

rewritten as

$$(\boldsymbol{I}_0 + \Delta\boldsymbol{I})\dot{\boldsymbol{\omega}} = -\boldsymbol{\Omega}(\boldsymbol{I}_0 + \Delta\boldsymbol{I})\boldsymbol{\omega} + \boldsymbol{M} + \Delta\varsigma \tag{2}$$

where $\boldsymbol{\omega} = [p \;\; q \;\; r]^{\mathrm{T}}$ is the angular velocity vector. $\Delta\boldsymbol{I}$ shows the uncertain parameters. The symbol $\Delta\varsigma$ represents the bounded disturbance in the dynamics equation.

Considering that the earth rotates slowly and that the vehicle moves at a high speed, the effect of the rotation of the earth is neglected. The translational movement is a long period movement. However, the attitude movement is a short period movement, so it is reasonable to ignore the influence of derivatives of velocity and position. Thus, the reentry vehicle kinematic equations are described as follows:

$$\dot{\alpha} = -p\cos(\alpha)\tan(\beta) + q - r\sin(\alpha)\tan(\beta) \tag{3}$$
$$\dot{\beta} = p\sin(\alpha) - r\cos(\alpha) \tag{4}$$
$$\dot{\sigma} = -p\cos(\alpha)\cos(\beta) - q\sin(\beta) - r\sin(\alpha)\cos(\beta) \tag{5}$$

where $\alpha$, $\beta$, $\sigma$ denote the angle of attack, sideslip angle, and bank angle, respectively.

Based on the above analysis, the attitude control model of the reentry vehicle can be described as follows:

$$\dot{\boldsymbol{\omega}} = -\boldsymbol{I}_0^{-1}\boldsymbol{\Omega}\boldsymbol{I}_0\boldsymbol{\omega} + \boldsymbol{I}_0^{-1}\boldsymbol{M} + \Delta\boldsymbol{d} \tag{6}$$
$$\dot{\boldsymbol{\theta}} = \boldsymbol{R}\boldsymbol{\omega} + \Delta\boldsymbol{f} \tag{7}$$

where $\boldsymbol{\theta} = [\alpha \;\; \beta \;\; \sigma]^{\mathrm{T}}$ and $\Delta\boldsymbol{f} = [\Delta f_1 \Delta f_2 \Delta f_3]^{\mathrm{T}}$ is the disturbances in the kinematic equations. $\Delta\boldsymbol{d} = [\Delta d_1 \Delta d_2 \Delta d_3]^{\mathrm{T}}$, which can be regarded as lumped disturbances, indicates the influence of the external environmental disturbances and parameters uncertainties in the dynamics equation. The specific expressions of $\Delta\boldsymbol{d}$ and $\boldsymbol{R}$ are shown as follows:

$$\Delta\boldsymbol{d} = \boldsymbol{I}_0^{-1}(-\Delta\boldsymbol{I}_0\dot{\boldsymbol{\omega}} - \boldsymbol{\Omega}\Delta\boldsymbol{I}\boldsymbol{\omega} + \Delta\varsigma) \tag{8}$$

$$\boldsymbol{R} = \begin{pmatrix} -\cos\alpha\tan\beta & 1 & -\sin\alpha\tan\beta \\ \sin\alpha & 0 & -\cos\alpha \\ -\cos\alpha\cos\beta & -\sin\beta & -\sin\alpha\cos\beta \end{pmatrix}$$

### B. THE TASK ANALYSIS OF ATTITUDE CONTROL SYSTEM

The task of the attitude control system is to control the attitude angles of the vehicle to track the desired signals, and to ensure that the vehicle completes the mission reliably under environmental disturbances. The attitude angle signals that need to be tracked are represented by $\boldsymbol{\theta}_d = [\alpha_d \;\; \beta_d \;\; \sigma_d]^{\mathrm{T}}$. By analyzing the movement of the reentry vehicle, the control system is divided into two loops for better control. The outer loop is the attitude angular tracking loop. And the inner loop is the angular velocity tracking loop. The terminal sliding mode controllers and nonlinear disturbance observers are designed for each loop. The outer loop generates the angular velocity command $\boldsymbol{\omega}_c$ required for system stability. The angular velocity command $\boldsymbol{\omega}_c$ is also treated as the commands needed to be tracked in the inner loop. The inner loop realizes the angular velocity commands $\boldsymbol{\omega}_c$ are tracked under the control torques $M$. The structure of attitude control system is shown in Fig. 1.

To analyse the problem conveniently, we make the following assumption:

*Assumption 1:* The derivatives of the disturbances are bounded, which means there are positive numbers $F_i$ and $D_i$ that satisfy max $|\Delta\dot{f}_i| < F_i$ and max $|\Delta\dot{d}_i| < D_i(i = 1,2,3)$.

## III. NONLINEAR DISTURBANCE OBSERVER DESIGN

A sliding mode observer(SMO) was proposed in [26], and a low pass filter is required during the estimation process. It is difficult to determine the cut-off frequency of the low-pass filter accurately, leading to the loss of observation accuracy. To make the estimated errors converge fast when the errors are large and converge within a finite time, new disturbance estimation laws inspired by [27] are proposed for reentry vehicles.

### A. DESIGN OF NONLINEAR DISTURBANCE OBSERVER FOR THE OUTER LOOP

For attitude angular tracking loop (7), the nonlinear disturbance observer is designed in the following form:

$$\dot{\hat{\boldsymbol{\theta}}} = \boldsymbol{R}\boldsymbol{\omega} + \Delta\hat{\boldsymbol{f}} \tag{9}$$
$$\Delta\hat{\boldsymbol{f}} = -\boldsymbol{k}_f\left|\hat{\boldsymbol{\theta}} - \boldsymbol{\theta}\right|^{\frac{1}{2}} sign(\hat{\boldsymbol{\theta}} - \boldsymbol{\theta}) + \boldsymbol{v}_1 \tag{10}$$

where $\hat{\boldsymbol{\theta}}$ represents the estimated value of $\boldsymbol{\theta}$, and $\Delta\hat{\boldsymbol{f}}$ is the estimated value of $\Delta\boldsymbol{f}$, $\boldsymbol{k}_f = diag\{k_{fi}\}$, $k_{fi} > 0$, $i = 1, 2, 3$, and $\boldsymbol{v}_1 = [v_{11}\ v_{12}\ v_{13}]^{\mathrm{T}}$ is an auxiliary control input designed as Eq. (11):

$$\dot{\boldsymbol{v}}_1 = -\boldsymbol{l}_1 sign(\hat{\boldsymbol{\theta}} - \boldsymbol{\theta}) - \boldsymbol{l}_2(\hat{\boldsymbol{\theta}} - \boldsymbol{\theta}) \tag{11}$$

where

$$\begin{aligned} sign(\boldsymbol{\theta}) &= [sign(\hat{\alpha} - \alpha)sign(\hat{\beta} - \beta)sign(\hat{\sigma} - \sigma)]^{\mathrm{T}} \\ &\in R^{3\times 1} \\ \left|\hat{\boldsymbol{\theta}} - \boldsymbol{\theta}\right|^{\frac{1}{2}} sign(\boldsymbol{\theta}) &= [\left|\hat{\alpha} - \alpha\right|^{\frac{1}{2}} sign(\hat{\alpha} - \alpha) \left|\hat{\beta} - \beta\right|^{\frac{1}{2}} \\ &\quad \times sign(\hat{\beta} - \beta) \left|\hat{\sigma} - \sigma\right|^{\frac{1}{2}} sign(\hat{\sigma} - \sigma)]^{\mathrm{T}} \\ &\in R^{3\times 1} \\ \boldsymbol{l}_1 &= diag\{l_{1i}\}, l_{1i} > 0, \quad \boldsymbol{l}_2 = diag\{l_{2i}\}, \\ l_{2i} &> 0, (i = 1, 2, 3). \end{aligned}$$

Before analyze the stability of the disturbance observer, we firstly introduce the definition of finite time convergence and the lemma of finite time convergence.

*Definition 1 [28]:* Consider the following nonlinear system:

$$\dot{x} = f(x, t) \quad f(0, t) = 0 \tag{12}$$

where $x \in R^y$ is the system state and $f : L \times R \to R$ is continuous on $L \times R$, where $L$ is an open neighbourhood of the origin . The origin is a finite time stable equilibrium point of system(12), if from any initial time $t_0$ and initial state $x_0$, there is a time $T(x_0) \geq 0$ that depends on $x_0$, such that the solution of system (12) satisfies the following conditions

$$\begin{cases} \lim\limits_{t\to T(x_0)} x(t, x_0) = 0 \\ x(t, x_0) = 0 \quad \forall t \geq T(x_0) \end{cases} \tag{13}$$

*Lemma 1 [29]:* For nonlinear systems (12), if there is a Lyapunov function $V$ that satisfies

1) $V$ is positive definite.
2)

$$\dot{V} + bV^{\gamma} \leq 0. \tag{14}$$

where $b > 0, 0 < \gamma < 1$,

the system states converge to the equilibrium point in finite time, and the setting time $t(x_0)$ depends on the initial system state $x(0) = x_0$, satisfying the following relationship:

$$t(x_0) \leq \frac{1}{b(1-\gamma)} V(x_0)^{1-\gamma} \tag{15}$$

*Theorem 1:* For the attitude angular tracking loop (7), by using the disturbance observers(9),(10), (11), and if parameters in observer that satisfy $k_{fi} > \sqrt{2F_i}$, $l_{1i} > 3F_i + \frac{2F_i^2}{k_{fi}^2}$, and $l_{2i} \geq 0$($F_i$ has been defined in Assumption 1), the disturbances estimation error can converge to zero within a finite time under Assumption 1.

*Proof:* From Eq. (7) and (9), we obtain:

$$\dot{\tilde{\boldsymbol{\theta}}} = \Delta\tilde{\boldsymbol{f}} = -\boldsymbol{k}_f \left|\hat{\boldsymbol{\theta}} - \boldsymbol{\theta}\right|^{\frac{1}{2}} sign(\hat{\boldsymbol{\theta}} - \boldsymbol{\theta}) + \boldsymbol{v}_1 - \Delta\boldsymbol{f} \tag{16}$$

where $\tilde{\boldsymbol{\theta}} = \hat{\boldsymbol{\theta}} - \boldsymbol{\theta} = [\tilde{\theta}_1\tilde{\theta}_2\tilde{\theta}_3]^T$ and $\Delta\tilde{\boldsymbol{f}}$ is the estimation error of disturbance where $\Delta\tilde{\boldsymbol{f}} = \Delta\hat{\boldsymbol{f}} - \Delta\boldsymbol{f}$.

The Lyapunov function is chosen as

$$V = \sum_{i=1}^{3} V_i \tag{17}$$

$$V_i = \boldsymbol{X}_i^T \boldsymbol{H}_i \boldsymbol{X}_i \tag{18}$$

where $\boldsymbol{X}_i = \left[\left|\tilde{\theta}_i\right|^{\frac{1}{2}} sign(\tilde{\theta}_i)\tilde{\theta}_i(v_{1i} - \Delta f_i)\right]^{\mathrm{T}} \in R^{3\times 1}$,

$$\boldsymbol{H}_i = \begin{bmatrix} 2l_{1i} + \frac{1}{2}k_{fi}^2 & 0 & -\frac{1}{2}k_{fi} \\ 0 & l_{2i} & 0 \\ -\frac{1}{2}k_{fi} & 0 & 1 \end{bmatrix}$$

when $k_{fi} > 0, l_{1i} > 0, l_{2i} > 0$, it can be verified that $\boldsymbol{H}_i$ is a positive definite matrix.

The above equation can be written as follow:

$$\begin{aligned} V = \sum_{i=1}^{i=3} \{ &\frac{1}{2}[k_{fi}\left|\tilde{\theta}_i\right|^{\frac{1}{2}} sign(\tilde{\theta}_i) - (v_{1i} - \Delta f_i)]^2 \\ &+ \frac{1}{2}(v_{1i} - \Delta f_i)^2 + 2l_{1i}(\left|\tilde{\theta}_i\right|^{\frac{1}{2}} sign(\tilde{\theta}))^2 + l_{2i}\tilde{\theta}_i^2\} \end{aligned} \tag{19}$$

Differentiating on both sides of Eq.(19), we can obtain:

$$\begin{aligned} \dot{V} = \sum_{i=1}^{i=3} &[k_{fi}\left|\tilde{\theta}_i\right|^{\frac{1}{2}} sign(\tilde{\theta}_i) - (v_{1i} - \Delta f_i)] \cdot [\frac{1}{2}k_{fi}\left|\tilde{\theta}_i\right|^{-\frac{1}{2}}\dot{\tilde{\theta}}_i \\ &- (\dot{v}_{1i} - \Delta\dot{f}_i)] + (v_{1i} - \Delta f_i)(\dot{v}_{1i} - \Delta\dot{f}_i) \\ &+ 2l_{1i}sign(\tilde{\theta}_i)\dot{\tilde{\theta}}_i + 2l_{2i}\tilde{\theta}_i\dot{\tilde{\theta}}_i \end{aligned} \tag{20}$$

Substituting Eq.(16) into Eq.(20), we can obtain:

$$\dot{V} = \sum_{i=1}^{3} -\frac{1}{\left|\tilde{\theta}_i\right|^{1/2}} \boldsymbol{X}_i^{\mathrm{T}} \boldsymbol{P}_i \boldsymbol{X}_i + \boldsymbol{X}_i^{\mathrm{T}} \begin{bmatrix} k_{fi}\Delta\dot{f}_i \\ 0 \\ -2\Delta\dot{f}_i \end{bmatrix} \tag{21}$$

where

$$\boldsymbol{P}_i = \begin{bmatrix} k_{fi}l_{1i} + \frac{1}{2}k_{fi}^3 & 0 & -\frac{1}{2}k_{fi}^2 \\ 0 & k_{fi}\boldsymbol{l}_{2i} & 0 \\ -\frac{1}{2}k_{fi}^2 & 0 & \frac{1}{2}k_{fi} \end{bmatrix}$$

Thus, the following relationship can be obtained:

$$\begin{aligned} \boldsymbol{X}_i^{\mathrm{T}} \begin{bmatrix} k_{fi}\Delta\dot{f}_i \\ 0 \\ -2\Delta\dot{f}_i \end{bmatrix} &= \left[\left|\tilde{\theta}_i\right|^{\frac{1}{2}} sign(\tilde{\theta}_i)\tilde{\theta}_i(v_{1i} - \Delta f_i)\right] \begin{bmatrix} k_{fi}\Delta\dot{f}_i \\ 0 \\ -2\Delta\dot{f}_i \end{bmatrix} \\ &= (k_{fi}\left|\tilde{\theta}_i\right|^{\frac{1}{2}} sign(\tilde{\theta}_i) - 2(v_{1i} - \Delta f_i))\Delta\dot{f}_i \\ &\leq k_{fi}F_i\left|\tilde{\theta}_i\right|^{\frac{1}{2}} - 2(v_{1i} - \Delta f_i)\Delta\dot{f}_i \end{aligned}$$

$$= \frac{1}{\left|\tilde{\theta}_i\right|^{1/2}} \boldsymbol{X}_i^T \boldsymbol{L}_i \boldsymbol{X}_i \tag{22}$$

The specific expressions of $\boldsymbol{L}_i$ is shown as follows:

$$\boldsymbol{L}_i = \begin{bmatrix} k_{fi}F_i & 0 & -\Delta\dot{f}_i sign(\tilde{\theta}_i) \\ 0 & 0 & 0 \\ -\Delta\dot{f}_{ii} sign(\tilde{\theta}_i) & 0 & 0 \end{bmatrix}$$

According to Eq.(21),(22), we can obtain the following inequality relationship:

$$\dot{V} \leq \sum_{i=1}^{3} -\frac{1}{|\theta_i|^{1/2}} \boldsymbol{X}_i^{\mathrm{T}} (\boldsymbol{P}_i - \boldsymbol{L}_i) \boldsymbol{X}_i \tag{23}$$

where

$$\boldsymbol{P}_i - \boldsymbol{L}_i = \begin{bmatrix} k_{fi}l_{1i} + \frac{1}{2}k_{fi}^3 - k_{fi}F_i & 0 & -\frac{1}{2}k_{fi}^2 + \Delta\dot{f}_i sign(\tilde{\theta}_i) \\ 0 & k_{fi}\boldsymbol{l}_{2i} & 0 \\ -\frac{1}{2}k_{fi}^2 + \Delta\dot{f}_i sign(\tilde{\theta}_i) & 0 & \frac{1}{2}k_{fi} \end{bmatrix}$$

When $(\boldsymbol{P}_i - \boldsymbol{L}_i)$ is positive definite matrix, the stability of the system can be guaranteed. We can know that if the following relationships are satisfied, $\boldsymbol{P}_i - \boldsymbol{L}_i$ is a positive definite matrix:

$$\begin{cases} k_{fi}l_{1i} + \frac{1}{2}k_{fi}^3 - k_{fi}F > 0 \\ (k_{fi}l_{1i} + \frac{1}{2}k_{fi}^3 - k_{fi}F_i)k_{fi}\boldsymbol{l}_{2i} > 0 \\ |\boldsymbol{P}_i - \boldsymbol{L}_i| > 0 \end{cases} \tag{24}$$

where $|\boldsymbol{P}_i - \boldsymbol{L}_i|$ is the determinant of $\boldsymbol{P}_i - \boldsymbol{L}_i$.

According to Eq.(24), we can obtain that if the following relationships are satisfied, $\boldsymbol{P}_i - \boldsymbol{L}_i$ is a positive definite matrix.

$$\begin{cases} k_{fi} > \sqrt{2F_i} \\ l_{1i} > 3F_i + \frac{2F_i^2}{k_{fi}^2} \\ l_{2i} > 0 \end{cases} \tag{25}$$

To accomplish the following proof, we define that $\rho_i$ is the minimum eigenvalue of the matrix $(\boldsymbol{P}_i - \boldsymbol{L}_i)$, and $h_i$ is the minimum eigenvalue of the matrix $\boldsymbol{H}_i$, thus, we can obtain:

$$\dot{V}_i \leq -\rho_{i\min} \frac{1}{\left|\tilde{\theta}_i\right|^{\frac{1}{2}}} \|X_i\|^2 \tag{26}$$

We can know that: $\|\boldsymbol{X}_i\|^2 \geq \frac{V_i}{h_{i\max}}, \frac{V_i}{h_{i\min}} \geq \|\boldsymbol{X}_i\|^2 \geq \left|\tilde{\boldsymbol{\theta}}_i\right|$, so the following relationship can be obtained:

$$\begin{aligned} \dot{V}_i &\leq -\rho_{i\min} \frac{V_i}{h_{i\max}} \frac{\sqrt{h_{i\min}}}{\sqrt{V_i}} \\ &= -\rho_{i\min} \frac{\sqrt{h_{i\min}}}{h_{i\max}} V_i^{\frac{1}{2}} \end{aligned} \tag{27}$$

We choose that:

$$\zeta = \min\{\rho_{1\min} \frac{\sqrt{h_{1\min}}}{h_{1\max}}, \quad \rho_{2\min} \frac{\sqrt{h_{2\min}}}{h_{2\max}}, \ \rho_{3\min} \frac{\sqrt{h_{3\min}}}{h_{3\max}}\}$$

From what is shown above, the following inequality can be obtained:

$$\dot{V} + \zeta V^{\frac{1}{2}} \leq 0 \tag{28}$$

According to Lemma 1, we can know that the state $\boldsymbol{X}_i$ converges to the origin within a finite time, so $\tilde{\boldsymbol{\theta}}$ and $\dot{\tilde{\theta}}$ converge to the origin within a finite time. And we can draw the conclusion by Eq.(16) that the estimation errors $\Delta\tilde{\boldsymbol{f}}$ converge to the origin in a finite time.

### B. DESIGN OF NONLINEAR DISTURBANCE OBSERVER FOR INNER LOOP

The nonlinear disturbance observer for inner control loop(6) is designed as follows:

$$\dot{\hat{\omega}} = -\boldsymbol{I}_0^{-1}\boldsymbol{\Omega}\boldsymbol{I}_0\boldsymbol{\omega} + \boldsymbol{I}_0^{-1}\boldsymbol{M} + \Delta\hat{\boldsymbol{d}} \tag{29}$$

$$\Delta\hat{\boldsymbol{d}} = -\boldsymbol{k}_d \left|\boldsymbol{v}_2\right|^{\frac{1}{2}} sign(\hat{\boldsymbol{\omega}} - \boldsymbol{\omega}) + \boldsymbol{v}_2 \tag{30}$$

where $\dot{\hat{\boldsymbol{\omega}}}$ and $\Delta\hat{\boldsymbol{d}}$ represent the estimated value of $\dot{\boldsymbol{\omega}}$ and $\Delta\boldsymbol{d}$, $\boldsymbol{k}_d = diag\{k_{di}\}$, $\boldsymbol{k}_{di} > 0$ and $\boldsymbol{v}_2 = [v_{21}\ v_{22}\ v_{23}]^{\mathrm{T}}$ is an auxiliary control vector that can be expressed as follows:

$$\dot{\boldsymbol{v}}_2 = -\boldsymbol{l}_3 sign(\hat{\boldsymbol{\omega}} - \boldsymbol{\omega}) - \boldsymbol{l}_4(\hat{\boldsymbol{\omega}} - \boldsymbol{\omega}) \tag{31}$$

where $\boldsymbol{l}_3 = diag\{l_{3i}\}, \boldsymbol{l}_4 = diag\{l_{4i}\}, \boldsymbol{l}_{3\mathrm{i}} > 0, \boldsymbol{l}_{4\mathrm{i}} > 0 (i = 1, 2, 3)$.

*Theorem 2:* For the system (6), by using the disturbance observers (29),(30), and (31), and if parameters are selected that satisfy $k_{di} > \sqrt{2_i D_i}$, $l_{3i} > 3D_i + \frac{2D_i^2}{k_{di}}$, $l_{4i} \geq 0$ ($D_i$ has been defined in Assumption 1), the disturbances estimation errors can converge within a finite time under Assumption 1.

The proof of Theorem 2 is omitted, which is similar to the proof of Theorem 1.

## IV. ADAPTIVE TERMINAL SLIDING MODE ATTITUDE CONTROL LAW DESIGN

### A. INTRODUCTION TO THE SUPER-TWIST CONTROL ALGORITHM

Before designing the controller, we introduce the following lemma, which is the core of the super-twist algorithm:

*Lemma 2 [23]:* For a class of nonlinear differential equation as follows:

$$\dot{s}(t) + k_1 \left|s(t)\right|^{\frac{1}{2}} sign(s(t)) + k_2 \int_0^t sign(s(t))dt = \eta(t) \tag{32}$$

where $k_1$ and $k_2$ are positive coefficients, and $\max|\dot{\eta}(t)| \leq C$, $C$ is a positive constant.

If parameters $k_1$ and $k_2$ satisfy the relationships that $k_1 \geq 1.5\sqrt{C}$ and $k_2 \geq 1.1C$, the solution of the differential equation (32) and its first order derivative will converge to zero within a finite time. Additionally, the variable $s$ moves to the origin in a smooth twisting way[30] shown in Fig. 2. The convergence time $T_r$ satisfies the following relationship:

$$T_r \leq \frac{7.6s(t_0)}{k_2 - C} \tag{33}$$

where $s(t_0)$ is the initial value of the variable $s$.

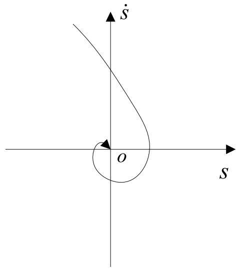


**FIGURE 2.** The motion trajectory of variable *s*.

So for an affine nonlinear system(34)

$$\dot{x} = f(x) + g(x)u + \zeta \tag{34}$$

where $x$ is the state of the system, and $f(x)$ is a continuous function, $g(x)$ is a continuous and invertible function. $\zeta$ is the disturbance in the system. To make the system state $x$ converge to the origin, we can design the control law $u$ shown as follow:

$$u = g(x)^{-1}(-f(x) - h_1 \left|x\right|^{\frac{1}{2}} sign(x) - h_2 \int_0^t sign(x)dt) \tag{35}$$

If the parameters $h_1$ and $h_2$ satisfy that $h_1 \geq 1.5\sqrt{\max\left|\dot{\zeta}\right|}$, $h_2 \geq 1.1 \max\left|\zeta\right|$, the stability of the system can be guaranteed according to Lemma 2. The design method of control law such as Eq. (35) is called the super-twist algorithm. The super-twist algorithm is proposed in sliding mode control, which is usually used to ensure that the sliding mode variable converges to the origin within a finite time. The control law(35) does not directly contain the sign function, which can weaken the chattering of the controller output.

### B. THE OUTER LOOP ADAPTIVE TERMINAL SLIDING MODE CONTROLLER DESIGN

For attitude angular control loop(7), a terminal sliding mode variable is designed as follows:

$$\boldsymbol{s}_1 = [s_{11} s_{12} s_{13}]^{\mathrm{T}} = \boldsymbol{\theta}_e + \int_0^t (\boldsymbol{a}_1 \boldsymbol{\theta}_e^{\frac{q_1}{p_1}} + \boldsymbol{b}_1 \boldsymbol{\theta}_e^m)dt \tag{36}$$

where $\boldsymbol{\theta}_e$ is the attitude angle tracking error vector that $\boldsymbol{\theta}_e = \boldsymbol{\theta} - \boldsymbol{\theta}_d$, $m > 1$ is a constant, $\boldsymbol{a}_1 = diag\{a_{11}, a_{12}, a_{13}\}$, $\boldsymbol{b}_1 = diag\{b_{11}, b_{12}, b_{13}\}$, $a_{ji}$ and $b_{ji} (j = 1, i = 1, 2, 3)$ are positive constants. $q_1$ and $p_2$ are positive odd integers, which satisfy the following inequality relationship:

$$0 < q_1 < p_1 < 2q_1 \tag{37}$$

Based on the sliding mode variable(36), the following adaptive sliding mode control law is designed:

$$\begin{cases} \boldsymbol{\omega}_c = \boldsymbol{R}^{-1}[\dot{\boldsymbol{\theta}}_d - \boldsymbol{a}_1 \boldsymbol{\theta}_e^{\frac{q_1}{p_1}} - \boldsymbol{b}_1 \boldsymbol{\theta}_e^m + \boldsymbol{\omega}_k - \Delta\hat{\boldsymbol{f}}] \\ \boldsymbol{\omega}_k = -\boldsymbol{k}_1 \left|\boldsymbol{s}_1\right|^{\frac{1}{2}} sign(\boldsymbol{s}_1) - \boldsymbol{k}_2 \int_0^t sign(\boldsymbol{s}_1)dt \end{cases} \tag{38}$$

where $\boldsymbol{k}_1 = diag\{k_{11}, k_{12}, k_{13}\}$, $\boldsymbol{k}_2 = diag\{k_{21}, k_{22}, k_{23}\}$ and $k_{ji} (j = 1, 2, i = 1, 2, 3)$ are positive constants.

*Theorem 3:* For the system(7), if the sliding variable(36) and the control law(38) are used, the sliding variable $\boldsymbol{s}_1$ will converge within a finite time. After the sliding mode variable $\boldsymbol{s}_1$ reaches the origin, the tracking errors converge within a finite time.

*Proof:* The proof of Theorem 3 is divided into two steps. The first step is to prove the convergence of the sliding mode variable $\boldsymbol{s}_1$. The second is to prove the convergence of angular tracking errors after the sliding mode variable converges to zero.

The differentiation of Eq.(36) can be available as:

$$\begin{aligned} \dot{\boldsymbol{s}}_1 &= \dot{\boldsymbol{\theta}}_e + \boldsymbol{a}_1 \boldsymbol{\theta}_e^{\frac{q_1}{p_1}} + \boldsymbol{b}_1 \boldsymbol{\theta}_e^m \\ &= \boldsymbol{R}\boldsymbol{\omega}_c + \Delta\boldsymbol{f} + \boldsymbol{a}_1 \boldsymbol{\theta}_e^{\frac{q_1}{p_1}} + \boldsymbol{b}_1 \boldsymbol{\theta}_e^m - \dot{\boldsymbol{\theta}}_d \end{aligned} \tag{39}$$

Substituting control law(38) into(39), we can obtain:

$$\dot{\boldsymbol{s}}_1 = -\boldsymbol{k}_1 \left|\boldsymbol{s}_1\right|^{\frac{1}{2}} sign(\boldsymbol{s}_1) - \boldsymbol{k}_2 \int_0^t sign(\boldsymbol{s}_1)dt + \Delta\boldsymbol{f} - \Delta\hat{\boldsymbol{f}} \tag{40}$$

Therefore, the following equation can be acquired:

$$\dot{\boldsymbol{s}}_1 + \boldsymbol{k}_1 \left|\boldsymbol{s}_1\right|^{\frac{1}{2}} sign(\boldsymbol{s}_1) + \boldsymbol{k}_2 \int_0^t sign(\boldsymbol{s}_1)dt = \Delta\boldsymbol{f} - \Delta\hat{\boldsymbol{f}} \tag{41}$$

From Theorem 1, it can be known that $\left\|\Delta\boldsymbol{f} - \Delta\hat{\boldsymbol{f}}\right\| \to 0$ within a finite time. Thus, according to Lemma 1, the value of parameter $\boldsymbol{k}_1$ and $\boldsymbol{k}_2$ can be selected as small to ensure that sliding mode variable $\boldsymbol{s}_1$ can converge within a finite time. Here, the super-twist algorithm is used to ensure that the terminal sliding mode variable $\boldsymbol{s}_1$ can converge to the origin.

After the sliding mode variable $\boldsymbol{s}_1$ converges, Eq.(36) is changed to:

$$\boldsymbol{\theta}_e + \int_0^t \boldsymbol{a}_1 \boldsymbol{\theta}_e^{\frac{q_1}{p_1}} + \boldsymbol{b}_1 \boldsymbol{\theta}_e^m dt = 0 \tag{42}$$

Differentiating on both sides of Eq.(42) results as:

$$\dot{\boldsymbol{\theta}}_e + \boldsymbol{a}_1 \boldsymbol{\theta}_e^{\frac{q_1}{p_1}} + \boldsymbol{b}_1 \boldsymbol{\theta}_e^m = 0 \tag{43}$$

Taking the angle of attack channel as an example, we can obtain:

$$\dot{\alpha}_e + a_{11} \alpha_e^{\frac{q_1}{p_1}} + b_{11} \alpha_e^m = 0 \tag{44}$$

where $\alpha_e = \alpha - \alpha_d$

Eq.(44) can be written as:

$$\dot{\alpha}_e = -a_{11} \alpha_e^{\frac{q_1}{p_1}} - b_{11} \alpha_e^m \tag{45}$$

The following equation can be obtained according to Eq.(45):

$$dt = \frac{d(\alpha_e)}{-(a_{11} \alpha_e^{\frac{q_1}{p_1}} + b_{11} \alpha_e^m)} \tag{46}$$

1) When the absolute value of the attitude angular tracking error is greater than one, the major part of the denominator in Eq.(46) is $-b_{11}\alpha_e^m$.

The time required for the error converging from initial value to one can be calculated as follows:

$$\begin{aligned} t_2 &= \int_{|\alpha_e(t_1)|}^{1} \frac{d(\alpha_e)}{-a_{11}\alpha_e^{\frac{q_1}{p_1}} - b_{11}\alpha_e^m} \\ &= \int_{1}^{|\alpha_e(t_1)|} \frac{d(\alpha_e)}{a_{11}\alpha_e^{\frac{q_1}{p_1}} + b_{11}\alpha_e^m} \\ &\le \int_{1}^{|\alpha_e(t_1)|} \frac{d(\alpha_e)}{b_{11}\alpha_e^m} \\ &= \frac{1}{b_{11}(m-1)}(1-|\alpha_e(t_1)|^{-m+1}) \end{aligned} \tag{47}$$

where $t_1$ is the time when the sliding mode variable converges to zero and $\alpha_e(t_1)$ is the attitude angle tracking error when the sliding mode variable converges.

2) When the value of the tracking error of attitude angle is smaller than one, the major part of the denominator in Eq.(46) is $-a_{11}\alpha_e^{\frac{q_1}{p_1}}$.

The time required for the error converging from one to zero is shown as follows:

$$\begin{aligned} t_3 &= \int_{1}^{0} \frac{d(\alpha_e)}{-a_{11}\theta_e^{\frac{q_1}{p_1}} - b_{11}\alpha_e^m} = \int_{0}^{1} \frac{d(\alpha_e)}{a_{11}\alpha_e^{\frac{q_1}{p_1}} + b_{11}\alpha_e^m} \\ &\le \int_{0}^{1} \frac{d(\alpha_e)}{a_1\alpha_e^{\frac{q_1}{p_1}}} = \frac{1}{a_{11}(-\frac{q_1}{p_1}+1)} = \frac{p_1}{a_{11}(p_1-q_1)} \end{aligned} \tag{48}$$

Thus, the total convergence time $T$ satisfies the following relationship:

$$T < t_1 + t_2 + t_3 \tag{49}$$

The analysis of the sideslip angle channel and the bank angle channel are similar to the angle of attack channel, which are omitted here.

The attitude angular control loop is a relative-degree- one system. The terminal sliding mode variable commonly used for relative-degree-one system is the integral terminal sliding mode variable $\sigma$ shown as follows[31]:

$$\sigma = e + a\int_0^t e^{\frac{q}{p}}dt \tag{50}$$

where $e$ represents the state tracking error, $a$ is a positive constant, $q$ and $p$ are positive odd integers which satisfy the relationship that $p > q > 0$.

When terminal sliding mode variable $\sigma$ keeps at the origin, we can obtain:

$$\dot{e} = -ae^{\frac{q}{p}} \tag{51}$$

Thus, the time $t$ need for $e$ converging to zero is:

$$t = \frac{|e(0)|}{a(1-\frac{q}{p})}^{1-\frac{q}{p}} \tag{52}$$

where $|e(0)|$ represents the initial state error.

According to the relationship between $q$ and $p$, we can know that $\frac{q}{p} < 1$. According to the above analysis based on the Eq.(46),(47),(48) and comparing the Eq.(45) and Eq.(51), we can get that error convergence faster using the terminal sliding mode variable designed in this paper than that using the sliding mode variable(50), which reflects the advantage of the sliding mode variable designed in this paper.

### C. The INNER ADAPTIVE TERMINAL SLIDING MODE CONTROLLER DESIGN

The inner loop is the angular velocity control loop. For inner loop(6), a terminal sliding mode variable is designed as follows:

$$\boldsymbol{s}_2 = [s_{21}s_{22}s_{23}]^{\mathrm{T}} = \boldsymbol{\omega}_e + \int_0^t (\boldsymbol{a}_2\boldsymbol{\omega}_e^{\frac{q_2}{p_2}} + \boldsymbol{b}_2\boldsymbol{\omega}_e^n)dt \tag{53}$$

where $\boldsymbol{\omega}_e$ is the angle velocity tracking error vector and $\boldsymbol{\omega}_e = \boldsymbol{\omega} - \boldsymbol{\omega}_c$, $n > 1$ is a constant. $\boldsymbol{a}_2 = diag\{a_{21}, a_{22}, a_{23}\}$, $\boldsymbol{b}_2 = diag\{b_{21}, b_{22}, b_{23}\}$ and $a_{ji}, b_{ji} (j = 2, i = 1, 2, 3)$ are positive constants. $q_2$ and $p_2$ are positive odd integers which satisfy the following inequality relationship:

$$0 < q_2 < p_2 < 2q_2 \tag{54}$$

The adaptive sliding mode control law designed based on sliding mode variable(53) is shown as follows:

$$\begin{cases} \boldsymbol{M} = \boldsymbol{I}_0[\dot{\boldsymbol{\omega}}_c + \boldsymbol{I}_0^{-1}\boldsymbol{\Omega}\boldsymbol{I}_0\boldsymbol{\omega} - \boldsymbol{a}_2\boldsymbol{\omega}_e^{\frac{q_2}{p_2}} - \boldsymbol{b}_2\boldsymbol{\omega}_e^n + \boldsymbol{M}_k - \Delta\hat{\boldsymbol{d}}] \\ \boldsymbol{M}_k = -\boldsymbol{k}_3\,|\boldsymbol{s}_2|^{\frac{1}{2}}\,sign(\boldsymbol{s}_2) - \boldsymbol{k}_4\int_0^t sign(\boldsymbol{s}_2)dt \end{cases} \tag{55}$$

where $\boldsymbol{k}_3 = diag\{k_{31}, k_{32}, k_{33}\}$, $\boldsymbol{k}_4 = diag\{k_{41}, k_{42}, k_{43}\}$ and $k_{ji}(j = 3, 4\ i = 1, 2, 3)$ are positive constants.

*Theorem 4:* For the system(6), if the sliding variable(53) and the control law(55) are applied, the sliding variable $\boldsymbol{s}_2$ will converge to zero under the designed control law. After the sliding mode variable $\boldsymbol{s}_2$ reaches the origin, the tracking errors converge within a finite time.

*Proof:* The proof of Theorem 4 is divided into two steps. The first step is to prove the convergence of the sliding mode variable $\boldsymbol{s}_2$, and the second is to prove the convergence of angular velocity tracking errors after the sliding mode variable $\boldsymbol{s}_2$ converges.

The differentiation of Eq.(53) can be available as follows:

$$\begin{aligned} \dot{\boldsymbol{s}}_2 &= \dot{\boldsymbol{\omega}}_e + \boldsymbol{a}_2\boldsymbol{\omega}_e^{\frac{q_2}{p_2}} + \boldsymbol{b}_2\boldsymbol{\omega}_e^n \\ &= -\boldsymbol{I}_0^{-1}\boldsymbol{\Omega}\boldsymbol{I}_0\boldsymbol{\omega} + \boldsymbol{I}_0^{-1}\boldsymbol{M} + \Delta\boldsymbol{d} + \boldsymbol{a}_2\boldsymbol{\omega}_e^{\frac{q_2}{p_2}} + \boldsymbol{b}_2\boldsymbol{\omega}_e^n - \dot{\boldsymbol{\omega}}_c \end{aligned} \tag{56}$$

Substituting control law(55) into(56), we can obtain:

$$\dot{\boldsymbol{s}}_2 = -\boldsymbol{k}_3\,|\boldsymbol{s}_2|^{\frac{1}{2}}\,sign(\boldsymbol{s}_2) - \boldsymbol{k}_4\int_0^t sign(\boldsymbol{s}_2)dt + \Delta\boldsymbol{d} - \Delta\hat{\boldsymbol{d}} \tag{57}$$

Therefore, the following equation can be acquired:

$$\dot{\boldsymbol{s}}_2 + \boldsymbol{k}_3\,|\boldsymbol{s}_2|^{\frac{1}{2}}\,sign(\boldsymbol{s}_2) + \boldsymbol{k}_4\int_0^t sign(\boldsymbol{s}_2)dt = \Delta\boldsymbol{d} - \Delta\hat{\boldsymbol{d}} \tag{58}$$

From Theorem 2, we can know that $\left\|\Delta\boldsymbol{d} - \Delta\hat{\boldsymbol{d}}\right\| \to 0$ within a finite time. Thus, the values of parameters $\boldsymbol{k}_3$ and $\boldsymbol{k}_4$

can be selected as small to ensure that sliding mode variable can converge in finite time according to Lemma 1.

The proof of angular velocity tracking errors converging within a finite time after sliding mode variable $\boldsymbol{s}_2$ converges is similar to the proof of Theorem 3.

*Remark 1:* The stability of the two loops is proved according to the above analysis. The outer loop generates the angular velocity command $\boldsymbol{\omega}_c$, which can be treated as the control input for the outer loop. When angular velocity command $\boldsymbol{\omega}_c$ can be responded to quickly by inner loop, it can be considered that the required angular velocities can be supplied to the outer loop fast and stably. In this way, the stability of the outer loop can be guaranteed, and the vehicle can track the desired attitude angles stably. This idea is similar to the idea of back-stepping. In order to ensure the stability of the system, the response speed of the inner loop should be faster than that of the outer loop, so the value of $k_{1i}$ should be chosen as ten times larger than $k_{3i}$, and the same relationship should exist between $k_{2i}$ and $k_{4i}(i = 1, 2, 3)$.

## V. NUMERICAL SIMULATION

In this part, in order to verify the effectiveness of the algorithm, numerical simulations are carried out using the proposed adaptive terminal sliding mode control (ATSMC). The physical parameters of the X-33 aircraft are used in the simulation.

The nominal inertia matrix $I_o$ is

$$\boldsymbol{I}_0 = \begin{bmatrix} 434270 & 0 & -17880 \\ 0 & 961200 & 0 \\ -17880 & 0 & 1131541 \end{bmatrix}$$

The parameters of the controllers are selected as follows:

$$\begin{aligned}
&\boldsymbol{k}_1 = diag\{0.2, 0.2, 0.2\}, \quad \boldsymbol{k}_2 = diag\{0.01, 0.01, 0.01\} \\
&\boldsymbol{k}_3 = diag\{18, 18, 18\}, \quad \boldsymbol{k}_4 = diag\{0.5, 0.5, 0.5\} \\
&m = 1.5, \quad n = 1.5 \\
&q1 = q2 = 7, \quad p1 = p2 = 9 \\
&\boldsymbol{a}_1 = diag\{4, 4, 4\}, \quad \boldsymbol{b}_1 = diag\{4, 4, 4\} \\
&\boldsymbol{a}_2 = diag\{4, 4, 4\}, \quad \boldsymbol{b}_2 = diag\{2, 2, 2\} \\
&\boldsymbol{l}_1 = diag\{0.8, 0.8, 0.8\}, \quad \boldsymbol{l}_2 = diag\{1, 1, 1\} \\
&\boldsymbol{l}_3 = diag\{5, 5, 5\}, \quad \boldsymbol{l}_4 = diag\{1, 1, 1\} \\
&\boldsymbol{k}_f = diag\{1, 1, 1\}, \quad \boldsymbol{k}_d = diag\{5, 5, 5\}
\end{aligned}$$

The initial states of the system are

$$\boldsymbol{\theta}_0 = [0^0, 10^0, 0^0]$$

To illustrate the effectiveness of the proposed algorithm, numerical simulations are performed in following two cases.

*Case 1:* In this case, the command signals are step signals, and the performance of the method proposed is compared to that of the integral sliding mode control(ISMC) and the integral terminal sliding mode control(ITSMC).

The integral sliding mode variables are presented as follows:

$$\boldsymbol{\sigma}_1 = \boldsymbol{\theta}_e + \int_0^t \boldsymbol{\theta}_e dt \tag{59}$$

$$\boldsymbol{\sigma}_2 = \boldsymbol{\omega}_e + \int_0^t \boldsymbol{\omega}_e dt \tag{60}$$

The integral sliding mode variable attitude control laws are shown as follows:

$$\boldsymbol{\omega}_c = \boldsymbol{R}^{-1}[\dot{\boldsymbol{\theta}}_d - \boldsymbol{\theta}_e - \boldsymbol{k}_{c1}\boldsymbol{\sigma}_1 - \boldsymbol{k}_{c2}sign(\boldsymbol{\sigma}_1)] \tag{61}$$

$$\boldsymbol{M} = \boldsymbol{I}_0[\dot{\boldsymbol{\omega}}_c + \boldsymbol{I}_0^{-1}\boldsymbol{\Omega}\boldsymbol{I}_0\boldsymbol{\omega} - \boldsymbol{\omega}_e - \boldsymbol{k}_{c3}\boldsymbol{\sigma}_2 - \boldsymbol{k}_{c4}sign(\boldsymbol{\sigma}_2)] \tag{62}$$

The parameters are chosen as:

$$\begin{aligned}
&\boldsymbol{k}_{c1} = diag\{0.2, 0.2, 0.2\}, \quad \boldsymbol{k}_{c2} = diag\{0.01, 0.01, 0.01\} \\
&\boldsymbol{k}_{c3} = diag\{18, 18, 18\}, \quad \boldsymbol{k}_{c4} = diag\{0.5, 0.5, 0.5\}
\end{aligned}$$

The ITSMC is designed based on the terminal sliding mode variable(50) and the super twist algorithm. And the parameter values of ITSMC are the same as that of ATSMC.

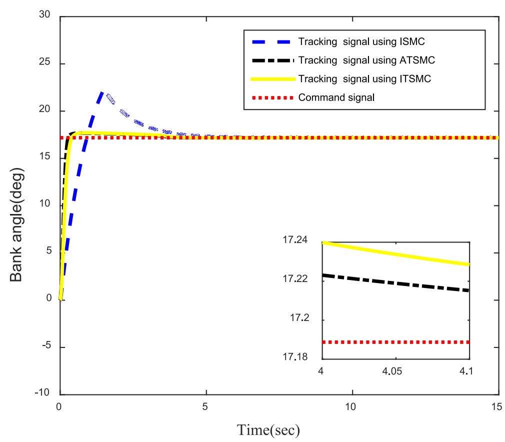


**FIGURE 3.** The response curve of angle of attack.

Comparisons between the adaptive terminal sliding mode control and ISMC, ITSMC are shown in Fig.3-7. It can be seen that all methods can ensure the angular tracking errors converge, but the errors convergence speed using ISMC is slower than using ATSMC and ITSMC. There is obvious overshoot in the tracking process using ISMC, which is not conducive to the stability of the vehicle. However, there is less overshoot in the tracking process by applying the ATSMC and ITSMC. It also can be obtained from the response curves of attitude angles that the tracking errors convergence speed using ATSMC is faster than that using ITSMC, which reflects the advantage of the terminal sliding mode variables designed. Comparing the control torque curve of two methods shown in Fig. 6 and Fig. 7, it is obvious that high frequency chattering exists in conventional integral sliding mode controller, which makes it difficult to be used in practical applications. The adaptive terminal sliding mode control law does not contain the sign function directly, and

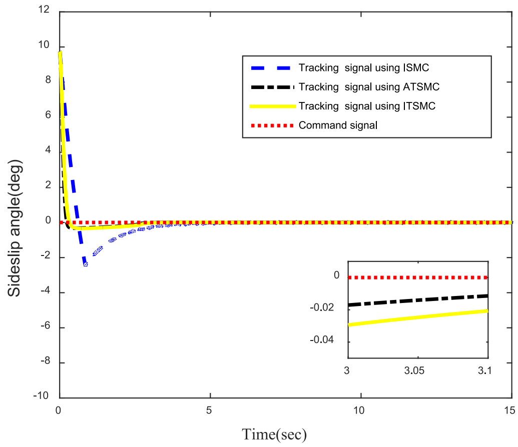


**FIGURE 4.** The response curve of sideslip angle.

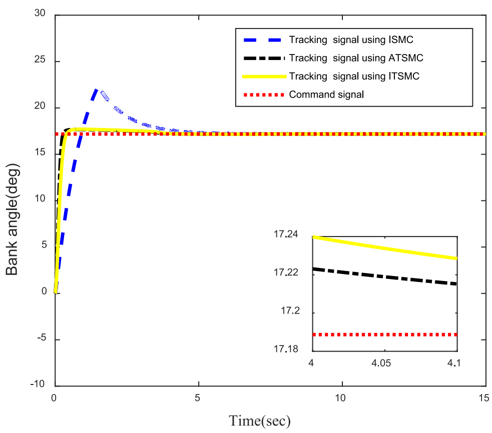


**FIGURE 5.** The response curve of bank angle.

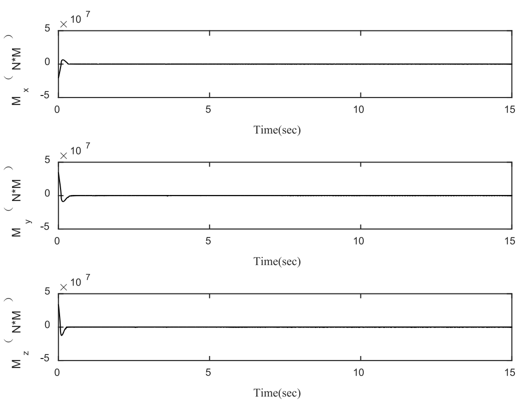


**FIGURE 6.** Control torque curve using ATSMC.

disturbances are effectively compensated, so the magnitude of chattering is reduced.

*Case 2:* In this case, the method proposed is used when the reentry vehicle makes large-scale maneuvers. The following disturbances, consisting of different frequency components, are added to the inner control loop and outer control loop after 12 seconds to simulate the influence of atmospheric changes

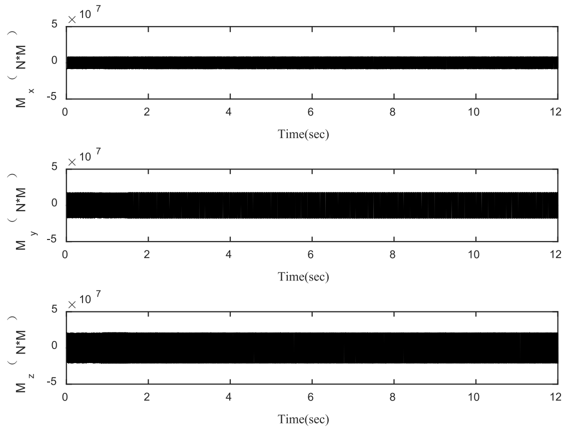


**FIGURE 7.** Control torque curve using ISMC.

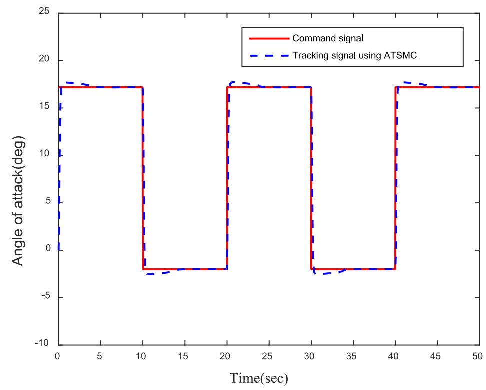


**FIGURE 8.** The response curve of angle of attack using ATSMC.

and parameter uncertainties on the flight process.

$$\Delta f = \begin{cases} 0.1+\sin(t)+\sin(t/5) \\ 0.1+\sin(t)+\sin(t/5) \\ 0.1+\sin(t)+\sin(t/5) \end{cases} \tag{63}$$

$$\Delta d = \begin{cases} 0.01+0.1\sin(t)+0.1\sin(t/5) \\ 0.01+0.1\sin(t)+0.1\sin(t/5) \\ 0.01+0.2\sin(t)+0.2\sin(t/5) \end{cases} \tag{64}$$

To prove the effectiveness of the nonlinear disturbance observer (NDO) proposed in section III. The extended state observer(ESO) proposed in [19] and the sliding mode observer(SMO) proposed in [26] are also used to estimate the disturbances in the inner loop.

The simulation results are shown in Fig. 8-20. The sideslip angle is generally maintained at 0 degrees during the reentry flight. The command signals of angle of attack and bank angle are square wave signals. According to the response process of the attitude angles, it can be known that with ATSMC, the vehicle can quickly track the desired attitude angle commands despite the presence of disturbances. With TSMC, there are tracking errors in the response process due to the influence of disturbances. According to the comparison test, we can know that using the disturbance observer can

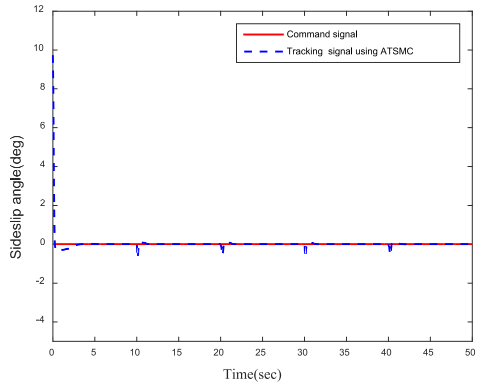


**FIGURE 9.** **The response curve of sideslip angle using ATSMC.**

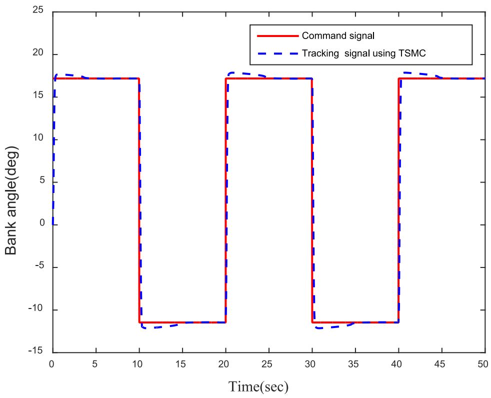


**FIGURE 10.** **The response curve of bank angle using ATSMC.**

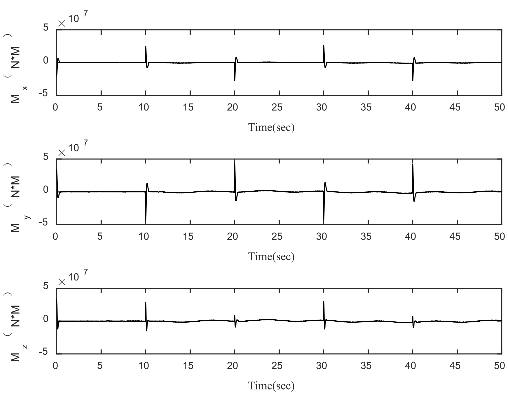


**FIGURE 11.** **Control torque curve using ATSMC.**

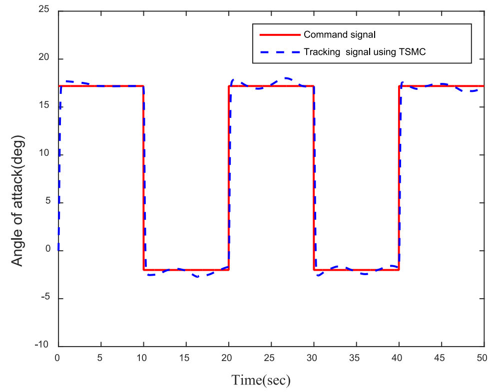


**FIGURE 12.** **The response curve of angle of attack using TSMC.**

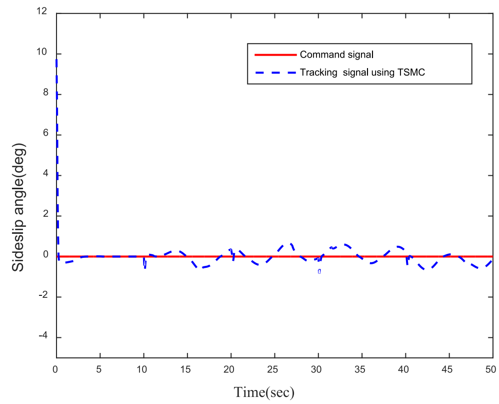


**FIGURE 13.** **The response curve of sideslip angle using TSMC.**

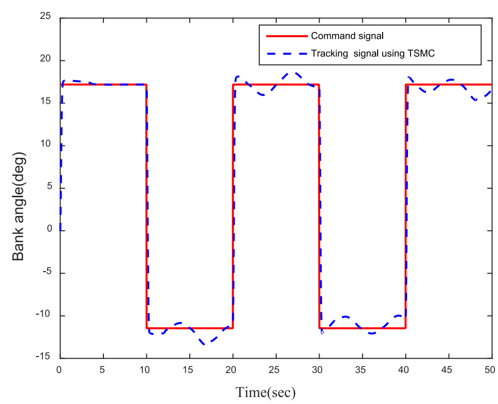


**FIGURE 14.** **The response curve of bank angle using TSMC.**

improve the robustness of the system, and the system can obtain higher tracking accuracy, which is beneficial for the vehicle to complete the flight mission. The strong robustness of the conventional sliding mode controller is at the expense of selecting large control gains, which will cause the controller output to generate high frequency chattering. And the robustness of the conventional sliding mode control is just to ensure the stability of the system. However, considering the estimated value of disturbances in the control laws can make the controllers compensate for disturbance adaptively and get good dynamic performance. At the same time, by using the nonlinear disturbance observers, smaller control gains are need to ensure the stability of the system, which is helpful to reduce the chattering of the controller output and guarantee the effectiveness of the actuators.

From Fig. 11, we can obtain that the vehicle can track the command signals effectively without significant chattering in the output of the controller. It can be known from Fig. 16 and Fig. 17 that the disturbances in two control loops are accurately estimated by using the disturbance observers proposed.

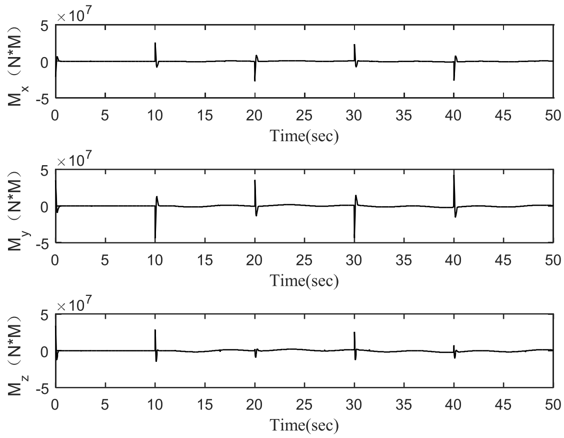


**FIGURE 15.** Control torque curve using TSMC.

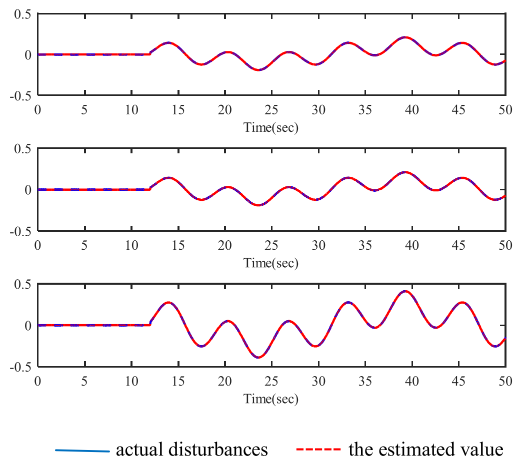


**FIGURE 16.** The estimated value of disturbances in outer loop by NDO.

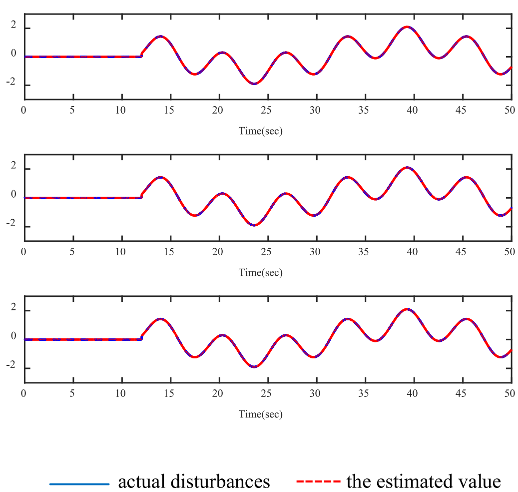


**FIGURE 17.** The estimated value of disturbances in inner loop by NDO.

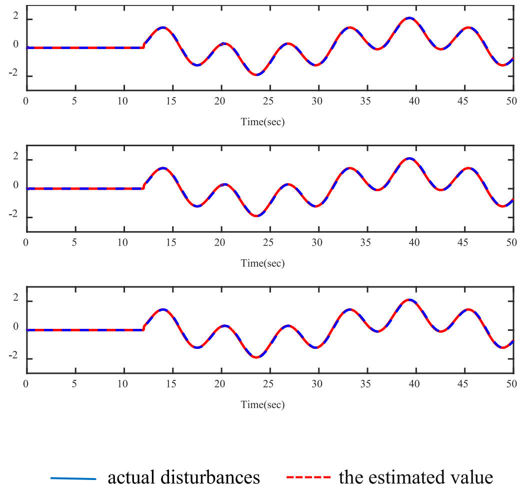


**FIGURE 18.** The estimated value of disturbances in inner loop by ESO.

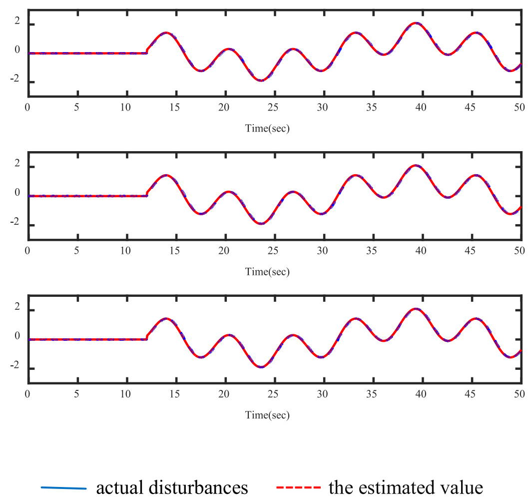


**FIGURE 19.** The estimated value of disturbances in inner loop by SMO.

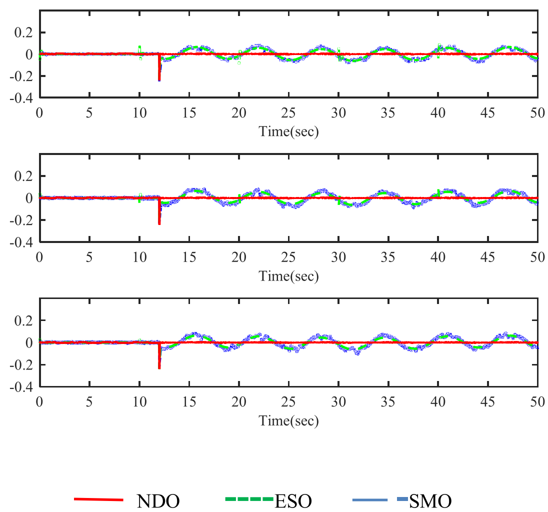


**FIGURE 20.** The estimated errors of disturbances in inner loop using NDO, ESO and SMO.

According to the estimated errors curve Fig. 20, it can be obtained that the observation error converges faster using the proposed NDO than using ESO and SMO, and there are no steady state errors by using NDO. The parametric selection of the extended state observer relies on experience, so to choose appropriate parameters for ESO requires more work than that for NDO. The low pass filter is required for SMO to reduce the chattering, which is not required for NDO.

## VI. CONCLUSION

To achieve an effective attitude control for reentry vehicles, an adaptive terminal sliding mode control law is proposed in this paper. First, the attitude control system is divided into an angular control loop and an angular velocities control loop. Then nonlinear disturbance observers are designed to obtain accurate estimations of the disturbances. The stability of the observer is analyzed by Lyapunov theory. Next, new terminal sliding mode control laws are proposed for each loop. The estimated values of the disturbance are used in the control laws to improve the anti-interference ability of the system. The control laws proposed are used to control the attitude of the reentry vehicle and are compared with the ISMC and TSMC in the same situation for comparisons. The performance of the proposed disturbance observers and controllers are illustrated via numerical simulations.

## REFERENCES


[1] Q. Mao, L. Dou, Q. Zong, and Z. Ding, "Attitude controller design for reusable launch vehicles during reentry phase via compound adaptive fuzzy H-infinity control," *Aerosp. Sci. Technol.*, vol. 72, pp. 36–48, Jan. 2018.

[2] W. Fang, Q. Zong, and D. Qi, "Robust adaptive attitude control of reentry vehicle with input constraint and uncertainty," in *Proc. 34th Chin. Control Conf. (CCC)*, Hangzhou, China, Jul. 2015, pp. 704–709.

[3] X. Shao and H. Wang, "Active disturbance rejection based trajectory linearization control for hypersonic reentry vehicle with bounded uncertainties," *ISA Trans.*, vol. 54, pp. 27–38, Jan. 2015.

[4] X. Shao and H. Wang, "Back-stepping robust trajectory linearization control for hypersonic reentry vehicle via novel tracking differentiator," *J. Franklin Inst.*, vol. 353, no. 9, pp. 1957–1984, Jun. 2016.

[5] B. H. An, Y. Wang, L. Liu, and Z. Hou, "An intelligent terminal sliding mode control algorithm with chattering reduction based on particle swarm optimization," in *Proc. 10th Int. Conf. Modelling, Identificat. Control (ICMIC)*, Guiyang, China, Jul. 2018, pp. 1–6.

[6] A. Levant, "Quasi-continuous high-order sliding-mode controllers," *IEEE Trans. Autom. Control*, vol. 50, no. 11, pp. 1812–1816, Nov. 2005.

[7] F. Muñoz, I. González-Hernández, S. Salazar, E. S. Espinoza, and R. Lozano, "SSecond order sliding mode controllers for altitude control of a quadrotor UAS: Real-time implementation in outdoor environments," *Neurocomputing*, vol. 233, no. C, pp. 61–71, Apr. 2017.

[8] B. Tian, W. Fan, Q. Zong, J. Wang, and F. Wang, "Nonlinear robust control for reusable launch vehicles in reentry phase based on time-varying high order sliding mode," *J. Franklin Inst.*, vol. 350, no. 7, pp. 1787–1807, Sep. 2013.

[9] B. Tian, Q. Zong, J. Wang, and F. Wang, "Quasi-continuous high-order sliding mode controller design for reusable launch vehicles in reentry phase," *Aerosp. Sci. Technol.*, vol. 28, no. 1, pp. 198–207, Jul. 2013.

[10] Y. Feng, X. Yu, and Z. Man, "Non-singular terminal sliding mode control of rigid manipulators," *Automatica*, vol. 38, no. 12, pp. 2159–2167, Dec. 2002.

[11] S. Yu, X. Yu, B. Shirinzadeh, and Z. Man, "Continuous finite-time control for robotic manipulators with terminal sliding mode," *Automatica*, vol. 41, no. 11, pp. 1957–1964, Nov. 2005.

[12] Y.-J. Wu, J.-X. Zuo, and L.-H. Sun, "Adaptive terminal sliding mode control for hypersonic flight vehicles with strictly lower convex function based nonlinear disturbance observer," *ISA Trans.*, vol. 71, pp. 215–226, Nov. 2017.

[13] N. Derbel, J. Ghommam, and Q. Zhu, "On the sliding control," in *Applications of Sliding Mode Control*, 1st ed. London, U.K.: Springer, 2017, pp. 10–26.

[14] S. R. Kumar, S. Rao, and D. Ghose, "Nonsingular terminal sliding mode guidance with impact angle constraints," *J. Guid., Control, Dyn.*, vol. 37, no. 4, pp. 1114–1130, Jun. 2014.

[15] C.-M. Lin and C.-F. Hsu, "Guidance law design by adaptive fuzzy sliding-mode control," *J. Guid., Control, Dyn.*, vol. 25, no. 2, pp. 248–256, Mar. 2012.

[16] P. Hušek and K. Narenathreyas, "Aircraft longitudinal motion control based on Takagi–Sugeno fuzzy model," *Appl. Soft. Comput.*, vol. 49, no. 2, pp. 269–278, Dec. 2016.

[17] Y. Shtessel, M. Taleb, and F. Plestan, "A novel adaptive-gain *supertwisting* sliding mode controller: Methodology and application," *Automatica*, vol. 48, no. 5, pp. 759–769, May 2012.

[18] Q. Dong, Q. Zong, B. Tian, and F. Wang, "Adaptive-gain multivariable super-twisting sliding mode control for reentry RLV with torque perturbation," *Int. J. Robust Nonlinear Control*, vol. 27, pp. 620–638, Mar. 2016.

[19] Z. Zhu, D. Xu, J. Liu, and Y. Xia, "Missile guidance law based on extended state observer," *IEEE Trans. Ind. Electron.*, vol. 60, no. 12, pp. 5882–5891, Dec. 2013.

[20] Y. Chen and B. Guo, "Sliding mode fault tolerant tracking control for a single-link flexible joint manipulator system," *IEEE Access*, vol. 7, pp. 83046–83057, 2019. doi: 10.1109/ACCESS.2019.2923789.

[21] H. Pan, W. Sun, H. Gao, and X. Jing, "Disturbance observer-based adaptive tracking control with actuator saturation and its application," *IEEE Trans. Autom. Sci. Eng.*, vol. 13, no. 2, pp. 868–875, Apr. 2016.

[22] H. Pan and W. Sun, "Nonlinear output feedback finite-time control for vehicle active suspension systems," *IEEE Trans. Ind. Informat.*, vol. 15, no. 4, pp. 2073–2082, Apr. 2019.

[23] C. E. Hall and Y. B. Shtessel, "Sliding mode disturbance observer-based control for a reusable launch vehicle," *J. Guid., Control, Dyn.*, vol. 29, no. 6, pp. 1315–1328, Nov. 2006.

[24] J. J. Recasens, Q. P. Chu, and J. A. Mulder, "Robust model predictive control of a feedback linearized system for a lifting-body re-entry vehicle," in *Proc. AIAA Guid., Navigat., Control Conf. Exhibit*, Aug. 2005, p. 6147.

[25] J. Geng, Y. Sheng, and X. Liu, "Finite-time sliding mode attitude control for a reentry vehicle with blended aerodynamic surfaces and a reaction control system," *Chin. J. Aeronaut.*, vol. 27, no. 4, pp. 964–976, Aug. 2014.

[26] G. Kenné, T. Ahmed-Ali, F. Lamnabhi-Lagarrigue, and A. Arzandé, "Nonlinear systems time-varying parameter estimation: Application to induction motors," *Electr. Power Syst. Res.*, vol. 78, no. 11, pp. 1881–1888, Nov. 2008.

[27] C. Sun, M. Zhao, and Z. Rui, *Terminal Mode Control Technology for Hypersonic Aircraft*. Nanjing, China: Science Press, 2014, pp. 117–147.

[28] Z. Zuo, Q.-L. Han, B. Ning, X. Ge, and X.-M. Zhang, "An Overview of Recent Advances in Fixed-Time Cooperative Control of Multi-Agent Systems," *IEEE Trans. Ind. Informat.*, vol. 14, no. 6, pp. 2322–2334, Jun. 2018.

[29] D. Zhou, S. Sun, and K. L. Teo, "Guidance laws with finite time convergence," *J. Guid., Control, Dyn.*, vol. 32, no. 6, pp. 1838–1846, Nov. 2009.

[30] Y. Shtessel, A. Levant, C. Edwards, and L. Fridman, *Sliding Mode Control and Observation*. New York, NY, USA, 2014, pp. 143–182.

[31] C. S. Chiu, "Derivative and integral terminal sliding mode control for a class of MIMO nonlinear systems," *Automatica*, vol. 48, no. 2, pp. 316–326, Feb. 2012.


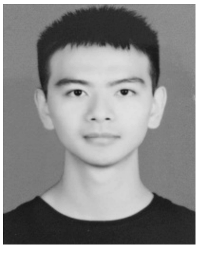

**BINGHE AN** received the bachelor's degree in mechatronic engineering from Huazhong Agricultural University, in 2017. He is currently pursuing the master's degree with the Huazhong University of Science and Technology.

His current research interests include sliding mode control and reinforcement learning.

**BO WANG** received the Ph.D. degree in electronic engineering from the University of Pretoria, South Africa, in 2017. He is currently a Lecturer with the Huazhong University of Science and Technology.

His current research interests include control theory and application, and intelligent optimization and control.

**YONGJI WANG** received the Ph.D. degree in power plant engineering from the Huazhong University of Science and Technology, in 1990.

He is currently a Professor with the Huazhong University of Science and Technology. His current research interests include control theory and application, aircraft control, and artificial neural networks.

**LEI LIU** received the Ph.D. degree in control science and engineering from the Huazhong University of Science and Technology, in 2009.

He is currently an Associate Professor with the Huazhong University of Science and Technology. His current research interests include aircraft control, trajectory planning, and optimization.